On Underweighting Nonlinear Measurements*

Renato Zanetti†

The Charles Stark Draper Laboratory, Houston, Texas 77058

Kyle J. DeMars‡ and Robert H. Bishop§

The University of Texas at Austin, Austin, Texas 78712

I. Introduction

The extended Kalman filter[1] (EKF) is a nonlinear approximation of the optimal linear Kalman filter.[2,3] In the presence of measurements that are nonlinear functions of the state, the EKF algorithm expands the filter's residual (difference between the actual measurement and the estimated measurement) in a Taylor series centered at the *a priori* state estimate. The EKF truncates the series to first-order, but second-order filters also exist.[4,5] It is well known that in the presence of highly accurate measurements the contribution of the second-order terms is essential when the *a priori* estimation error covariance is large.[5,6] Possible solutions include implementing a second-order Gaussian filter[5] or an unscented Kalman filter (UKF).[7] The UKF is a nonlinear extension to the Kalman filter capable of retaining the second moments (or higher) of the estimation error distribution. Even when retaining the second-order terms of the Taylor series, the methods still rely on an approximation and therefore good filtering results may not always be achievable. Historically, second-order filters are not used because of their computational cost. The Space Shuttle, for example, utilizes an *ad hoc* technique known as underweighting.[8,9]

The commonly implemented method for the underweighting of measurements for human space navigation was introduced by Lear[10] for the Space Shuttle navigation system. In 1966 Denham and Pines showed the possible inadequacy of the linearization approximation

*Presented as paper AAS 09-367 at the 2009 AAS/AIAA Astrodynamics Specialist Conference.

†Senior Member of the Technical Staff, GN&C Manned Space Systems, 17629 El Camino Real, Suite 470, rzanetti@draper.com, AIAA Member.

‡PhD Student, Department of Aerospace Engineering and Engineering Mechanics, 210 East 24th Street, W. R. Woolrich Laboratories, 1 University Station, demarskj@mail.utexas.edu, AIAA Member.

§Professor, Department of Aerospace Engineering and Engineering Mechanics, 210 East 24th Street, W. R. Woolrich Laboratories, 1 University Station, rhbishop@mail.utexas.edu, AIAA Fellow.

when the effect of measurement nonlinearity is comparable to the measurement error.[11] To compensate for the nonlinearity Denham and Pines proposed to increase the measurement noise covariance by a constant amount. In the early seventies, in anticipation of Shuttle flights, Lear and others developed relationships which accounted for the second-order effects in the measurements.[8] It was noted that in situations involving large state errors and very precise measurements, application of the standard extended Kalman filter mechanization leads to conditions in which the state estimation error covariance decreases more rapidly than the actual state errors. Consequently the extended Kalman filter begins to ignore new measurements even when the measurement residual is relatively large. Underweighting was introduced to slow down the convergence of the state estimation error covariance thereby addressing the situation in which the error covariance becomes overly optimistic with respect to the actual state errors. The original work on the application of second-order correction terms led to the determination of the underweighting method by trial-and-error.[10]

More recently, studies on the effects of nonlinearity in sensor fusion problems with application to relative navigation have produced a so-called "bump-up" factor.[12–15] While Ferguson[12] seems to initiate the use of the bump-up factor, the problem of mitigating filter divergence was more fully studied by Plinval[13] and subsequently by Mandic.[14] Mandic generalized Plinval's bump-up factor to allow flexibility and notes that the value selected influences the steady-state convergence of the filter. In essence, it was found that a larger factor keeps the filter from converging to the level that a lower factor would permit. This finding prompted Mandic to propose a two-step algorithm in which the bump-up factor is applied for a certain number of measurements only, upon which the factor was completely turned off. Finally, Perea, et al.[15] summarize the findings of the previous works and introduce several ways of computing the applied factor. In all cases, the bump-up factor amounts in application to the underweighting factor introduced in Lear.[10] Save for the two-step procedure of Mandic, the bump-up factor is allowed to persistently affect the Kalman gain which directly influences the obtainable steady-state covariance. Effectively, the ability to remove the underweighting factor autonomously and under some convergence condition was not introduced.

While of great historical importance, the work of Lear is not well known as it is only documented in internal NASA memos.[8,10] Kriegsman and Tau[9] mention underweighting in their 1975 Shuttle navigation paper without a detailed explanation of the technique. The purpose of this note is to review the motivations behind underweighting and to document its historical introduction. Lear's scheme uses a single scalar coefficient and tuning is necessary in order to achieve good performance. A new method for determining the underweighting factor is introduced, together with an automated method for deciding when the underweighting factor should and should not be applied. By using the Gaussian approximation and bounding

the second-order contributions, suggested values for the coefficient are easily obtained. The proposed technique has the advantage of Lear's scheme's simplicity combined with the theoretical foundation of the Gaussian second-order filter. The result yields a simple algorithm to aid the design of the underweighted EKF.

II. Need for Underweighting

We review briefly the three state estimate update approaches assuming a linear time-varying measurement model leading to the classical Kalman filter, a nonlinear measurement model with first-order linearization approximations leading the widely used extended Kalman filter, and a nonlinear model with second-order approximations leading to the second-order extended Kalman filter.

A. Linear Measurement Model and the Classical Kalman Filter Update

In the classical linear setting associated with the development of optimal state estimation using the Kalman filter,[1] consider the measurement model given by

$$\mathbf{y}_k = \mathbf{H}_k \mathbf{x}_k + \boldsymbol{\eta}_k \,, \tag{1}$$

where $\mathbf{y}_k \in \mathbb{R}^m$ are the m measurements at each time t_k, $\mathbf{x}_k \in \mathbb{R}^n$ is the n-dimensional state vector, $\mathbf{H}_k \in \mathbb{R}^{m\times n}$ is the known measurement mapping matrix, $\boldsymbol{\eta}_k \in \mathbb{R}^m$ is modeled as a zero-mean white-noise sequence with $\mathrm{E}\left\{\boldsymbol{\eta}_k\right\} = 0$, $\forall\ k$ and $\mathrm{E}\left\{\boldsymbol{\eta}_k \boldsymbol{\eta}_j^{\mathrm{T}}\right\} = \mathbf{R}_k \delta_{kj}$ where $\mathbf{R}_k > 0$ $\forall\ k$ and $\delta_{kj} = 1$ when $k = j$ and $\delta_{kj} = 0$ when $k \neq j$. The Kalman filter state update algorithm provides an optimal blending of the *a priori* estimate $\hat{\mathbf{x}}_k^-$ and the measurement $\mathbf{y}_k$ at time t_k to obtain the *a posteriori* state estimate $\hat{\mathbf{x}}_k^+$ via

$$\hat{\mathbf{x}}_k^+ = \hat{\mathbf{x}}_k^- + \mathbf{K}_k \left[\mathbf{y}_k - \mathbf{H}_k \hat{\mathbf{x}}_k^-\right] \,, \tag{2}$$

where the superscript $^-$ denotes *a priori* and $^+$ denotes *a posteriori*.

Defining the *a priori* estimation error as $\mathbf{e}_k^- = \mathbf{x}_k - \hat{\mathbf{x}}_k^-$ and the *a posteriori* estimation error as $\mathbf{e}_k^+ = \mathbf{x}_k - \hat{\mathbf{x}}_k^+$ and assuming these errors to be zero mean, the associated symmetric, positive definite *a priori* and *a posteriori* estimation error covariances are $\mathbf{P}_k^- = \mathrm{E}\left\{\mathbf{e}_k^- \left(\mathbf{e}_k^-\right)^{\mathrm{T}}\right\}$ and $\mathbf{P}_k^+ = \mathrm{E}\left\{\mathbf{e}_k^+ \left(\mathbf{e}_k^+\right)^{\mathrm{T}}\right\}$, respectively. Using Eq. (2) and the definitions of the state estimation errors and error covariances, we obtain the *a posteriori* state estimation error covariance via the well-known Joseph formula

$$\mathbf{P}_k^+ = \left[\mathbf{I} - \mathbf{K}_k \mathbf{H}_k\right] \mathbf{P}_k^- \left[\mathbf{I} - \mathbf{K}_k \mathbf{H}_k\right]^{\mathrm{T}} + \mathbf{K}_k \mathbf{R}_k \mathbf{K}_k^{\mathrm{T}} \,, \tag{3}$$

which is valid for any $\mathbf{K}_k$. If the gain $\mathbf{K}_k$ is chosen so as to minimize the trace of the *a posteriori* estimation error, we call that gain the Kalman gain and it is given by

$$\mathbf{K}_k = \mathbf{P}_k \mathbf{H}_k^{\mathrm{T}} \left[\mathbf{H}_k \mathbf{P}_k^- \mathbf{H}_k^{\mathrm{T}} + \mathbf{R}_k \right]^{-1} . \tag{4}$$

The trace of the state estimation error covariance is generally not a norm but is equivalent to the nuclear norm (the matrix Shatten 1-norm) for symmetric semi-positive matrices. If the gain given in Eq. (4) is applied to the state estimation error covariance of Eq. (3), then the update equation can be rewritten after some manipulation as

$$\mathbf{P}_k^+ = \left[\mathbf{I} - \mathbf{K}_k \mathbf{H}_k \right] \mathbf{P}_k^- , \tag{5}$$

or equivalently,

$$\mathbf{P}_k^+ = \mathbf{P}_k^- - \mathbf{K}_k [\mathbf{H}_k \mathbf{P}_k^- \mathbf{H}_k^{\mathrm{T}} + \mathbf{R}_k] \mathbf{K}_k^{\mathrm{T}} . \tag{6}$$

Under the assumptions of the Kalman filter development (linear, time-varying measurement model with a zero-mean white-noise sequence corrupting the measurements, unbiased *a priori* estimation errors, known dynamics and measurement models, etc.), the state estimate and state estimation error covariance updates are optimal and we expect no filter divergence issues. The estimation error covariance will remain positive definite for all t_k and the estimation error covariance will be consistent with the true errors. In practice, the measurements are generally better represented with nonlinear measurement models leading to a variety of engineering solutions, mostly *ad hoc*, that must be carefully designed to ensure acceptable state estimation performance. Underweighting is one such method to improve the performance of the extended Kalman filter in practical settings.

B. Nonlinear Measurement Model and the Extended Kalman Filter Update

In the nonlinear setting, consider the measurement model given by

$$\mathbf{y}_k = \mathbf{h}(\mathbf{x}_k) + \boldsymbol{\eta}_k , \tag{7}$$

where $\mathbf{h}(\mathbf{x}_k) \in \mathbb{R}^m$ is a vector-valued differentiable nonlinear function of the state vector $\mathbf{x}_k \in \mathbb{R}^n$. The idea behind the extended Kalman filter (EKF) is to utilize Taylor series approximations to obtain linearized models in such a fashion that the EKF state update algorithm has the same general form as the Kalman filter. To that end, we find that the state estimate update is given by[1]

$$\hat{\mathbf{x}}_k^+ = \hat{\mathbf{x}}_k^- + \mathbf{K}_k [\mathbf{y}_k - \mathbf{h}(\hat{\mathbf{x}}_k^-)] . \tag{8}$$

Following the usual extended Kalman filter development procedure of using Taylor series expansions about the *a priori* state estimate (and neglecting higher-order terms), we find the measurement residual is given by

$$\boldsymbol{\epsilon}_k = \mathbf{y}_k - \mathbf{h}(\hat{\mathbf{x}}_k^-) \simeq \mathbf{H}_k \mathbf{e}_k^- + \boldsymbol{\eta}_k \,, \tag{9}$$

where

$$\mathbf{H}_k \triangleq \left[\left. \frac{\partial \mathbf{h}(\mathbf{x}_k)}{\partial \mathbf{x}_k} \right|_{\mathbf{x}_k = \hat{\mathbf{x}}_k^-} \right] . \tag{10}$$

Computing the measurement residual covariance $\mathrm{E}\left\{\boldsymbol{\epsilon}_k \boldsymbol{\epsilon}_k^{\mathrm{T}}\right\}$ yields

$$\mathbf{W}_k = \mathbf{H}_k \mathbf{P}_k^- \mathbf{H}_k^{\mathrm{T}} + \mathbf{R}_k \,. \tag{11}$$

The state estimation error covariance and Kalman gain are the same as in Eqs. (3) and (4), respectively, with $\mathbf{H}_k$ given as in Eq. (10). The state estimation error covariances in the forms shown in Eqs. (5) and (6) also hold in the nonlinear setting with $\mathbf{H}_k$ as in Eq. (10).

From Eqs. (6) and (8), it is seen that reducing the Kalman gain leads to a smaller update in both the state estimation error covariance and the state estimate, respectively. Reducing the gain is the essence of underweighting and the need for this adjustment is illuminated in the following discussion.

Adopting the viewpoint that the state estimation error covariance matrix represents the level of uncertainty in the state estimate, we expect that when we process a measurement (representing new information) that the uncertainty would decrease (or at least, not increase). This is, in fact, the case and can be seen in Eq. (6). Under the assumption that the symmetric matrices $\mathbf{P}_k^- > 0$ and $\mathbf{R}_k > 0$, it follows that

$$\mathbf{K}_k[\mathbf{H}_k \mathbf{P}_k^- \mathbf{H}_k^{\mathrm{T}} + \mathbf{R}_k]\mathbf{K}_k^{\mathrm{T}} \geq 0 \,, \tag{12}$$

and we can find a number $\alpha_k \geq 0$ at each time t_k such that

$$\mathbf{P}_k^- - \mathbf{P}_k^+ \geq \alpha_k \mathbf{I} \,, \tag{13}$$

which shows that the $\mathbf{P}_k^- - \mathbf{P}_k^+$ is non-negative definite. The same argument can be made from the viewpoint of comparing the trace (or the matrix norm) of the *a posteriori* and *a priori* state estimation error covariances. As each new measurement is processed by the EKF, we expect the uncertainty in the estimation error to decrease. The question is, does the *a posteriori* uncertainty as computed by the EKF represent the actual uncertainty, or in other words, is the state estimation error covariance matrix always consistent with the actual

state errors? In the nonlinear setting when there is a large *a priori* uncertainty in the state estimate and a very accurate measurement, it can happen that the state estimation error covariance reduction at the measurement update is too large. The underweighting discussed here is a method to address this situation by limiting the magnitude of the state estimation error covariance update with the goal of retaining consistency of the filter covariance and the actual state estimation errors.

Pre- and post-multiplying the *a posteriori* state estimation error covariance in Eq. (6) by $\mathbf{H}_k$ and $\mathbf{H}_k^{\mathrm{T}}$, respectively, yields (after some manipulation)

$$\mathbf{H}_k\mathbf{P}_k^{+}\mathbf{H}_k^{\mathrm{T}} = \mathbf{H}_k\mathbf{P}_k^{-}\mathbf{H}_k^{\mathrm{T}}(\mathbf{H}_k\mathbf{P}_k^{-}\mathbf{H}_k^{\mathrm{T}} + \mathbf{R}_k)^{-1}\mathbf{R}_k\,. \tag{14}$$

In Eq. (14), we see that if $\mathbf{H}_k\mathbf{P}_k^{-}\mathbf{H}_k^{\mathrm{T}} \gg \mathbf{R}_k$ then it follows that

$$\mathbf{H}_k\mathbf{P}_k^{+}\mathbf{H}_k^{\mathrm{T}} \simeq \mathbf{R}_k\,. \tag{15}$$

The result in Eq. (15) is of fundamental importance and is the motivation behind underweighting.

C. Nonlinear Measurement Model and the 2nd-Order Kalman Filter Update

Consider the nonlinear measurement model in Eq. (7) and assume the state update is given by

$$\hat{\mathbf{x}}_k^{+} = \hat{\mathbf{x}}_k^{-} + \mathbf{K}_k(\mathbf{y}_k - \hat{\mathbf{y}}_k)\,. \tag{16}$$

We compute the measurement residual following the usual extended Kalman filter development procedure of using Taylor series expansions about the *a priori* state estimate except that we now keep up to second-order terms in the Taylor series expansion. Let $\mathbf{b}_k$ represent the second-order term of the Taylor series expansion of $\mathbf{h}(\mathbf{x}_k)$. Define

$$\mathbf{H}'_{i,k} \triangleq \left[\left.\frac{\partial^2 h_i(\mathbf{x}_k)}{\partial\mathbf{x}_k\partial\mathbf{x}_k^{\mathrm{T}}}\right|_{\mathbf{x}_k=\hat{\mathbf{x}}_k^{-}}\right],$$

where $h_i(\mathbf{x}_k)$ is the i^{th} component of $\mathbf{h}(\mathbf{x}_k)$. Then the i^{th} component of $\mathbf{b}_k$ is given by

$$b_{i,k} = \frac{1}{2}\,(\mathbf{e}_k^{-})^{\mathrm{T}}\mathbf{H}'_{i,k}\mathbf{e}_k^{-} = \frac{1}{2}\,\mathrm{trace}(\mathbf{H}'_{i,k}\mathbf{e}_k^{-}(\mathbf{e}_k^{-})^{\mathrm{T}})\,. \tag{17}$$

To keep the filter unbiased the measurement estimate in Eq. (16) is chosen as

$$\hat{\mathbf{y}}_k = \mathbf{h}(\hat{\mathbf{x}}_k^{-}) + \hat{\mathbf{b}}_k\,, \tag{18}$$

where the i^{th} component of $\hat{\mathbf{b}}_k$ is given by

$$\hat{b}_{i,k} = 1/2\,\mathrm{trace}(\mathbf{H}'_{i,k}\mathbf{P}_k^-)\,.$$

The measurement residual is defined as

$$\boldsymbol{\epsilon}_k = \mathbf{y}_k - \hat{\mathbf{y}}_k. \tag{19}$$

Expanding Eq. (19), the i^{th} component of the residual is obtained to be

$$\epsilon_{i,k} = \mathbf{H}_{i,k}\,\mathbf{e}_k^- + 1/2\,\mathrm{trace}(\mathbf{H}'_i(t_k)\mathbf{e}_k^-(\mathbf{e}_k^-)^{\mathrm{T}}) - 1/2\,\mathrm{trace}(\mathbf{H}'_i(t_k)\mathbf{P}_k^-) + \eta_{i,k}\,, \tag{20}$$

where $\mathbf{H}_{i,k}$ is the i^{th} row of the measurement Jacobian and $\eta_{i,k}$ is the i^{th} component of the measurement noise $\boldsymbol{\eta}_k$. Computing the measurement residual covariance $\mathrm{E}\left\{\boldsymbol{\epsilon}_k\boldsymbol{\epsilon}_k^{\mathrm{T}}\right\}$ yields

$$\mathbf{W}_k = \mathbf{H}_k\mathbf{P}_k^-\mathbf{H}_k^{\mathrm{T}} + \mathbf{B}_k + \mathbf{R}_k\,, \tag{21}$$

where matrix $\mathbf{B}_k$ is the contribution of the second order effects and its ij^{th} component is given by

$$\begin{aligned} B_{ij,\,k} \triangleq\; & 1/4\,\mathrm{E}\left\{\mathrm{trace}(\mathbf{H}'_i(t_k)\mathbf{e}_k^-(\mathbf{e}_k^-)^{\mathrm{T}})\ \mathrm{trace}(\mathbf{H}'_i(t_k)\mathbf{e}_k^-(\mathbf{e}_k^-)^{\mathrm{T}})\right\} \\ & - 1/4\ \mathrm{trace}(\mathbf{H}'_i(t_k)\mathbf{P}_k^-)\ \mathrm{trace}(\mathbf{H}'_i(t_k)\mathbf{P}_k^-)\,. \end{aligned}$$

Under the Gaussian approximation, the ij^{th} component of $\mathbf{B}_k$ is given by

$$B_{ij,\,k} = \frac{1}{2}\,\mathrm{trace}(\mathbf{H}'_j(t_k)\,\mathbf{P}_k^-\,\mathbf{H}'_i(t_k)\,\mathbf{P}_k^-)\,. \tag{22}$$

Comparing the measurement residual covariance for the EKF in Eq. (11) with the measurement residual covariance for the second-order filter in Eq. (21), we see that when the nonlinearities lead to significant second-order terms which should not be neglected, then the EKF tends to provide state estimates that are not consistent with the actual errors. Typically, we address this by tuning the EKF using $\mathbf{R}_k$ and the process noise (not discussed here but part of the propagation phase of the EKF) as parameters to be tweaked. If the contribution of the *a priori* estimation error $\mathbf{H}_k\mathbf{P}_k^-\mathbf{H}_k^{\mathrm{T}}$ to the residuals covariance is much larger than the contribution of the measurement error $\mathbf{R}_k$, the EKF algorithm will produce $\mathbf{H}_k\mathbf{P}_k^+\mathbf{H}_k^{\mathrm{T}} \simeq \mathbf{R}_k$. If $\mathbf{B}_k$ is of comparable magnitude to $\mathbf{R}_k$ then the actual $\mathbf{H}_k\mathbf{P}_k^+\mathbf{H}_k^{\mathrm{T}} \simeq \mathbf{R}_k + \mathbf{B}_k$. Therefore, a large underestimation of the *a posteriori* covariance can occur in the presence of nonlinearities when the estimated measurement error covariance is much larger than the measurement error covariance.

The covariance update is given by the modified Gaussian second order filter update[4]

$$\mathbf{P}_k^+ = \mathbf{P}_k^- - \mathbf{H}_k\mathbf{P}_k^-\mathbf{W}_k^{-1}\left(\mathbf{H}_k\mathbf{P}_k^-\right)^{\mathrm{T}}, \tag{23}$$

where the residual covariance $\mathbf{W}_k$ is given by Eq. (21).

III. Underweighting Measurements

Underweighting is the process of modifying the residual covariance to reduce the update and compensate for the second-order effects described above. In this section, we describe three common methods for performing underweighting with the EKF algorithm.

A. Additive Compensation Method

The most straightforward underweighting scheme is to add an underweighting factor $\mathbf{U}_k$ as

$$\mathbf{W}_k = \mathbf{H}_k\mathbf{P}_k^-\mathbf{H}_k^{\mathrm{T}} + \mathbf{R}_k + \mathbf{U}_k\,. \tag{24}$$

With the Kalman gain given by

$$\mathbf{K}_k = \mathbf{P}_k^-\mathbf{H}_k^{\mathrm{T}}\mathbf{W}_k^{-1}\,, \tag{25}$$

we see that the symmetric, positive-definite underweighting factor $\mathbf{U}_k$ decreases the Kalman gain, thereby reducing the state estimate and state estimation error covariance updates. One choice is to select $\mathbf{U}_k = \mathbf{B}_k$, which is, for example, the current design for the Orion vehicle.[16] The advantage of this choice is its theoretical foundation based on analyzing the second-order terms of the Taylor series expansions. The disadvantages include higher computational costs to calculate the second-order partials and the reliance on the assumption that the estimation errors possess Gaussian distributions. In practical applications, the matrix $\mathbf{U}_k$ needs to be tuned appropriately for acceptable overall performance of the EKF. The process of tuning a positive definite matrix is less obvious than tuning a single scalar parameter.

B. Scaling the Measurement Error Covariance

Another possible underweighting approach is to scale the measurement noise by choosing

$$\mathbf{U}_k = \beta\mathbf{R}_k\,, \tag{26}$$

where $\beta > 0$ is a scalar parameter selected in the design process. This approach has been successfully used;[17] however, it is not recommended from both a conceptual and a practical

reason. Recalling that the underweighting is necessary because of neglecting the second-order terms of the Taylor series expansion of the measurement function, it seems more natural to express the underweighting as a function of the *a priori* estimation error covariance. Choosing a constant coefficient to scale $\mathbf{R}_k$ seems less practical and will probably lead to a more complicated tuning procedure.

C. Lear's Method

Lear's choice was to make $\mathbf{U}_k$ a percentage of the *a priori* estimation error covariance via[10]

$$\mathbf{U}_k = \beta \mathbf{H}_k \mathbf{P}_k^- \mathbf{H}_k^{\mathrm{T}} \,. \tag{27}$$

Let $\bar{\mathbf{P}}_k^- \in \mathbb{R}^{3\times 3}$ be the partition of the state estimation error covariance associated with the position error states. The Space Shuttle employs underweighting when $\sqrt{\operatorname{trace} \bar{\mathbf{P}}_k^-} > \alpha$. The positive scalars α and β are design parameters. For the Space Shuttle, α is selected to be 1000 meters and β is selected to be 0.2.[10] When $\sqrt{\operatorname{trace} \bar{\mathbf{P}}_k^-} > 1000$ m, then $\beta = 0.2$, otherwise $\beta = 0$.

IV. Tuning Aids

In this section, a technique to aid the tuning of the underweighting coefficient is presented. When the nonlinearities lead to second-order terms that cannot be neglected, we find that the measurement residual covariance is more accurately given by (see Eq. (21))

$$\mathbf{W}_k = \mathbf{H}_k \mathbf{P}_k^- \mathbf{H}_k^{\mathrm{T}} + \mathbf{R}_k + \mathbf{B}_k \,. \tag{28}$$

Following Lear's approach to underweighting the measurement residual covariance, we propose an underweighting of the form

$$\mathbf{W}_{U,k} = (1 + \beta_k) \mathbf{H}_k \mathbf{P}_k^- \mathbf{H}_k^{\mathrm{T}} + \mathbf{R}_k \,. \tag{29}$$

Comparing Eqs. (28) and (29), the desired effect is to have

$$\operatorname{trace} \mathbf{W}_{U,k} \geq \operatorname{trace} \mathbf{W}_k \quad \forall\, k \,. \tag{30}$$

This leads us to choose the underweighting coefficient β_k such that

$$\beta_k \geq \operatorname{trace} \mathbf{B}_k / \operatorname{trace} \mathbf{H}_k \mathbf{P}_k^- \mathbf{H}_k^{\mathrm{T}} \,. \tag{31}$$

On the surface, this approach does not have any great advantage over the additive compensation method where we choose $\mathbf{U}_k = \mathbf{B}_k$ since $\mathbf{B}_k$ needs to be calculated in both cases. However, often a bound on the Hessian of the measurement function exists, therefore it is not necessary to compute the second-order term of the Taylor series expansion. It is known that the j^{th} term on the diagonal of $\mathbf{B}$ at time t_k is bounded by[18]

$$B_{jj,\,k} \leq \frac{1}{2}\left(\|\mathbf{H}'_{j,k}\| \operatorname{trace} \mathbf{P}_k^-\right)^2 , \tag{32}$$

where $\|\cdot\|$ indicates the matrix or vector 2-norm. Therefore, it follows that

$$\operatorname{trace} \mathbf{B}_k \leq \frac{1}{2}(\operatorname{trace} \mathbf{P}_k^-)^2 \sum_{j=1}^{m} \|\mathbf{H}'_{j,k}\|^2 \leq \frac{c_k}{2}(\operatorname{trace} \mathbf{P}_k^-)^2 , \tag{33}$$

where c_k is an upper bound of $\sum_{j=1}^{m} \|\mathbf{H}'_{j,k}\|^2$. If we select β_k as

$$\beta_k = \frac{c_k}{2} \frac{(\operatorname{trace} \mathbf{P}_k^-)^2}{\operatorname{trace} \mathbf{H}_k \mathbf{P}_k^- \mathbf{H}_k^{\mathrm{T}}} , \tag{34}$$

then the inequality in Eq. (31) is satisfied at any t_k. Based on previous discussions, the underweighting should be applied when the nonlinearities are such that the second-order terms in the Taylor series expansion are comparable in magnitude to the measurement noise. A good rule of thumb in determining when underweighting should be applied is

$$\frac{c_k}{2}(\operatorname{trace} \mathbf{P}_k^-)^2 > z \operatorname{trace} \mathbf{R}_k , \tag{35}$$

where $0 < z < 1$ is a parameter to be specified. Since $\mathbf{P}_k^- > 0$, the relationship in Eq. (35) is equivalent to

$$\operatorname{trace} \mathbf{P}_k^- > \left(\frac{2z}{c_k} \operatorname{trace} \mathbf{R}_k\right)^{1/2} . \tag{36}$$

Notice that Eq. (36) is similar to Lear's rule on when to apply underweight in that the check depends on computing the trace of the *a priori* state estimation error covariance. In this case, however, Eq. (34) is derived using upper bounds that could be artificially loose if precautions are not taken. An artificially loose upper bound could negate the positive contribution of the underweighting method proposed here to obtain a good design value for β_k. The suggested precaution is to only include in the computation of the trace of $\mathbf{P}_k^-$ the states that actually contribute to the measurement. This is similar to Lear's method in which only the trace of the state estimation error covariance associated with the position states are included in the computation. Of course, Lear was considering the spacecraft rendezvous problem and this was a sensible precaution given the measurements from the Shuttle rendezvous radar.

V. Numerical Results

Consider a two spacecraft system with a non-maneuvering target vehicle and a chaser vehicle maneuvering in proximity. The principle relative sensor is a LIDAR (Light Detection And Ranging) measuring the range and two bearing angles from the chaser to the target. The chaser vehicle also has an IMU (inertial measurement unit) providing measurements of velocity changes (due to non-gravitational sources) and changes in attitude, and an on-board GPS system. The range measurement at t_k is modeled as the range between the two vehicles $\rho_k = \|\mathbf{r}_{rel,k}\|$. The Jacobian (with respect to position only) is given by

$$\mathbf{H}_k = \frac{1}{\rho_k}\,\mathbf{r}_{rel,k}^{\mathrm{T}}\,.$$

The Hessian (with respect to relative position only) is given by

$$\mathbf{H}'_k = \frac{1}{\rho_k}\left(\mathbf{I} - \mathbf{r}_{rel,k}\mathbf{r}_{rel,k}^{\mathrm{T}}/\rho_k^2\right) = -\frac{1}{\rho_k^3}[\mathbf{r}_{rel,k}\times]^2\,.$$

The matrix $\mathbf{H}'_k$ is symmetric with a zero eigenvalue and a repeated eigenvalue at $1/\rho_k$. The norm of the Hessian does not need to be bounded because is known analytically $\|\mathbf{H}'_k\| = 1/\rho_k$. Out of the three LIDAR measurements, the range is the bigger contributor to the second order effects, therefore the upper bound c_k is chosen as $3/\rho_k^2$. The LIDAR is activated when the two vehicles are 1 km apart. The chaser EKF filter is initialized with a GPS update of the chaser state and a ground update of the target state. The GPS accuracy is assumed 10 m per axis (1σ) the ground update is assumed to have accuracy 20 m per axis (1σ).

The LIDAR measurement is corrupted by normally distributed random noise and a random constant bias. The LIDAR range noise and bias are assumed to be range dependent, varying linearly from 0.01 m at docking to 0.1 m (1σ) at a relative distance of 100 meters. For any range greater than 100 meters the noise and bias are fixed to the maximum value of 0.1 m (1σ). It is assumed that the LIDAR takes 2 minutes to scan its entire field of view and that two scans are required for reacquisition. We simulate a loss of track scenario in which the LIDAR is tracking nominally for about 1.3 hours before a loss of track leading to a 4 minute gap in LIDAR measurements. The performance of the EKF with and without underweighting is examined.

Figures 1 and 2 show the performance of the EKF filter without underweighting for a set of 100 monte carlo runs. Each plot contains the 100 actual state estimation errors (gray lines) and the the square root of the diagonal elements of the filter's covariance for each of the 100 runs (black lines, 3σ). Figure 3 zooms in the position error after loss of track. It can be seen that when the EKF reacquires (after the 4 minute delay for the two

LIDAR scans) the uncertainty in the state estimate (as measured by the EKF covariance) rapidly decreases. However, in many of the samples the actual state errors do not decrease as quickly leading to an inconsistency in the state errors and the state estimation error covariance. Therefore, when the next measurement becomes available the predicted state estimation error covariance of the residual is small and the measurement is rejected because the actual measurement residual is more than 5 times its predicted standard deviation. In the absence of residual editing, i.e. if the measurements are accepted regardless of how large the measurement residuals are, the EKF would diverge. When measurements are rejected, the filter only propagates and the state estimation error covariance will continue to increase. In either case, the performance of the EKF is unacceptable. From Figure 3 it can be seen that in a few runs the covariance snaps back down some time after re-acquisition. Because of the rejections, the propagation-only phase causes the covariance to increase. In certain cases, the added uncertainty is sufficient to eventually accept measurements. Figure 3 also shows many diverging cases. In a well-designed filter, the estimation error should match the predicted covariance, and the filter should not reject measurements after re-acquisition. The filter's covariance should rapidly decrease after re-acquisition and stay small for the remainder of the simulation.

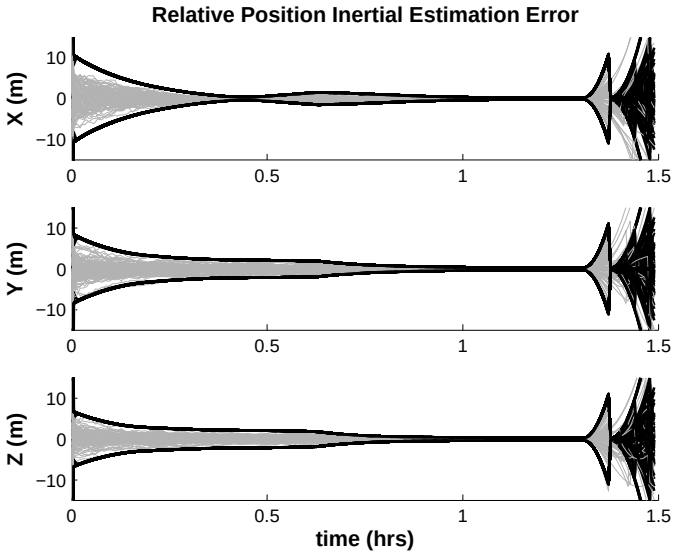

Figure 1. Relative Position Performance without Underweighting.

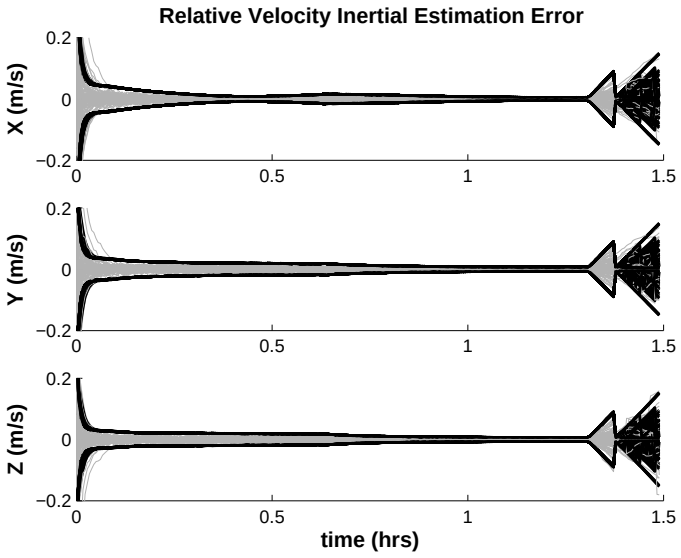

Figure 2. Relative Velocity Performance without Underweighting.

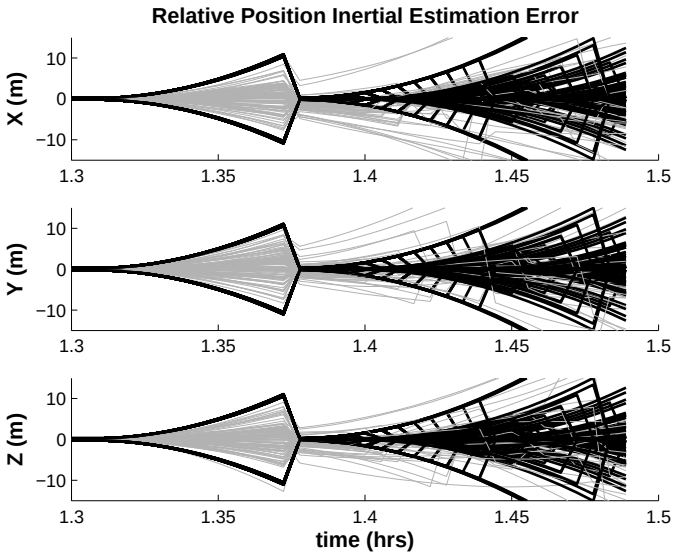

Figure 3. Relative Position Performance without Underweighting.

Figures 4 and 5 show the results when underweighting is applied. The underweighting coefficient is chosen using Eq. (34) and it is applied when the condition of Eq. (36) is satisfied with $z = 0.1$ in Eq. (35). Following the suggested precaution discussed in the previous section, we include only the relative position states in the computation of the trace $\mathbf{P}_k^-$. The covariance update is given by Eq. (23) by substituting $\mathbf{B}_k$ with $\beta_k \mathbf{H}_k \mathbf{P}_k^- \mathbf{H}_k^{\mathrm{T}}$ and rewriting it in an equivalent Joseph formula-like form

$$\mathbf{P}_k^+ = [\mathbf{I} - \mathbf{K}_k \mathbf{H}_k]\, \mathbf{P}_k^- \, [\mathbf{I} - \mathbf{K}_k \mathbf{H}_k]^{\mathrm{T}} + \mathbf{K}_k (\beta_k \mathbf{H}_k \mathbf{P}_k^- \mathbf{H}_k^{\mathrm{T}} + \mathbf{R}_k) \mathbf{K}_k^{\mathrm{T}} \,.$$

It can be seen in Figures 4 and 5 that the proposed underweighting method allows the EKF to re-converge after the LIDAR begins to provide measurements again.

From Figures 4 and 5 it can be seen that all 100 samples of the filter's covariance are nearly on top of one another. Figures 6 and 7 show one realization of the covariance (1σ, solid line) versus the sample covariance calculated from the estimation errors of the 100 runs (1σ, dashed line). It can be seen that the two lines are closely superimposed, demonstrating the filter's covariance is consistent with the actual estimation error's uncertainty.

VI. Conclusions

In this note the purpose of underweighting is reviewed. The original underweighting scheme by Lear is introduced. Other existing schemes are discussed. Techniques to aid the choice of the tuning parameters of Lear's underweighting schemes are introduced. A numerical example showing the need for underweighting and the performance of the pro-

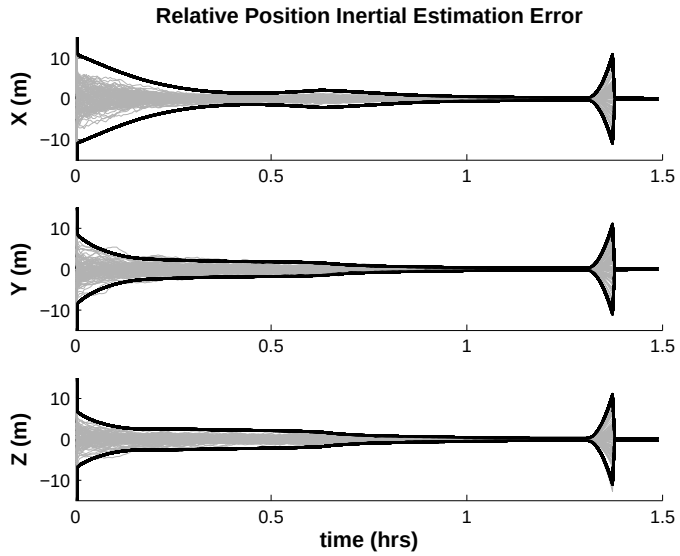

Figure 4. Relative Position Performance with Underweighting.

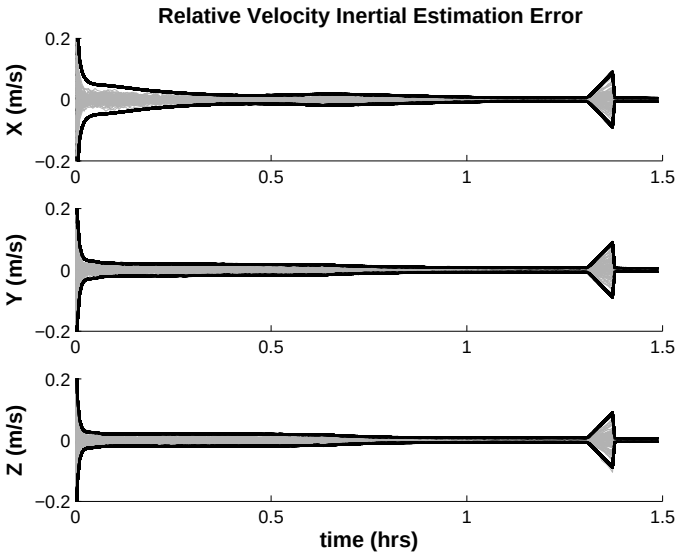

Figure 5. Relative Velocity Performance with Underweighting.

posed method is illustrated. The numerical results suggest that the proposed solution is a viable method to tune the underweighted extended Kalman filter in the presence of LIDAR measurements.

References

[1]Gelb, A., editor, *Applied Optimal Estimation*, The MIT Press, Cambridge, MA, 1974.

[2]Kalman, R. E., "A New Approach to Linear Filtering and Prediction Problems," *Transactions of the*

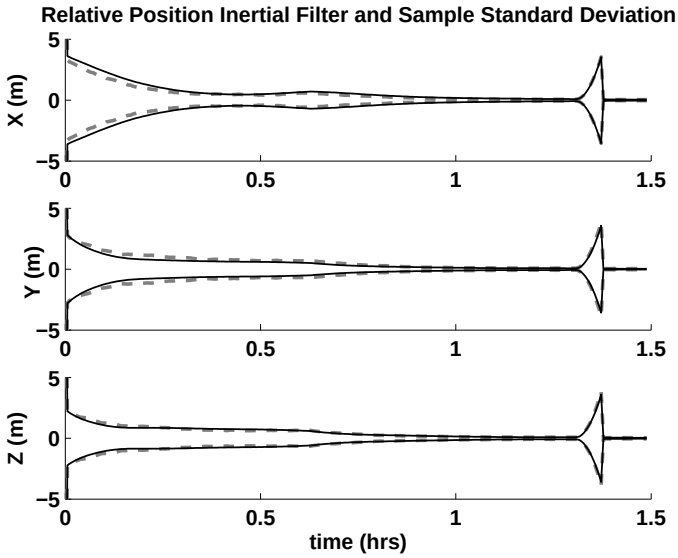

Figure 6. Relative Position Consistency with Underweighting.

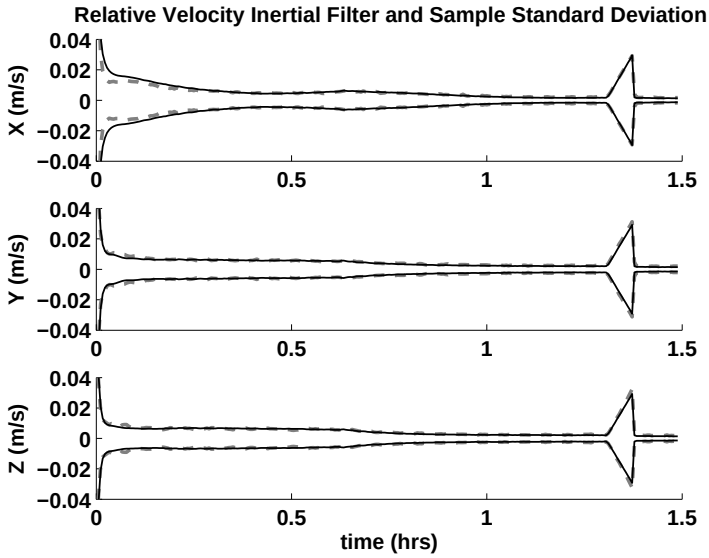

Figure 7. Relative Velocity Consistency with Underweighting.

ASME – Journal of Basic Engineering, Vol. 82, 1960, pp. 35–45.

[3]Kalman, R. E. and Bucy, R. S., "New Results in Linear Filtering and Prediction," *Journal of Basic Engineering*, 1961, pp. 83–95.

[4]Jazwinski, A. H., *Stochastic Processes and Filtering Theory*, Dover, 2007.

[5]Maybeck, P. S., *Stochastic Models, Estimation, and Control*, Vol. 2, Academic Press, 1982.

[6]Huxel, P. J. and Bishop, R. H., "Fusing Inertial and Relative Measurements for Inertial Navigation in the Presence of Large State Error Covarianaces," *Proceedings of the 16th AAS/AIAA Spaceflight Mechanics Meeting*, January 2006.

[7]Julier, S. J. and Uhlmann, J. K., "A New Extension of the Kalman Filter to Nonlinear Systems," *Int.*

Symp. Aerospace/Defense Sensing, Simul. and Controls, Orlando, FL, 1997.

[8]Lear, W. M., "Kalman Filtering Techniques," Tech. Rep. JSC-20688, NASA Johnson Space Center, Houston, TX, 1985.

[9]Kriegsman, B. A. and Tau, Y. C., "Shuttle Navigation System for Entry and Landing Mission Phases," *Journal of Spacecraft*, Vol. 12, No. 4, April 1975, pp. 213–219.

[10]Lear, W. M., "Multi-Phase Navigation Program for the Space Shuttle Orbiter," Internal Note No. 73-FM-132, NASA Johnson Space Center, Houston, TX, 1973.

[11]Denham, W. F. and Pines, S., "Sequential Estimation when Measurement Function Nonlinearity is Comparable to Measurement Error," *AIAA Journal*, Vol. 4, No. 6, June 1966, pp. 1071–1076.

[12]Ferguson, P. and How, J., "Decentralized Estimation Algorithms for Formation Flying Spacecraft," *AIAA Guidance, Navigation and Control Conference*, 2003.

[13]Plinval, H., *Analysis of Relative Navigation Architectures for Formation Flying Spacecraft*, Master's thesis, Massachusetts Institute of Technology, 2006.

[14]Mandic, M., *Distributed Estimation Architectures and Algorithms for Formation Flying Spacecraft*, Master's thesis, Massachusetts Institute of Technology, 2006.

[15]Perea, L., How, J., Breger, L., and Elosegui, P., "Nonlinearity in Sensor Fusion: Divergence Issues in EKF, modified truncated SOF, and UKF," *AIAA Guidance, Navigation and Control Conference and Exhibit*, Hilton Head, SC, August 20–23, 2007.

[16]Hanak, C. and Zanetti, R., "Relative Navigation of the Orion Vehicle," *Proceedings of the F. Landis Markley Astronautics Symposium held June 30 – July 2, 2008, Cambridge, MD*, Vol. 132 of *Advances in the Astronautical Sciences*, 2008, pp. 793–811, AAS 08-306.

[17]Jenkins, S. C. and Geller, D. K., "State Estimation and Targeting for Autonomous Rendezvous and Proximity Operations," *Proceedings of the AAS/AIAA Astrodynamics Specialists Conference*, Mackinac Island, MI, August 19–23 2007.

[18]Huxel, P. J. and Bishop, R. H., "Navigation Algorithms and Observability Analysis for Formation Flying Missions," *Journal of Guidance, Control, and Dynamics*, Vol. 32, No. 4, July–August 2009, pp. 1218–1231.